

# RSC Advances



This is an *Accepted Manuscript*, which has been through the Royal Society of Chemistry peer review process and has been accepted for publication.

*Accepted Manuscripts* are published online shortly after acceptance, before technical editing, formatting and proof reading. Using this free service, authors can make their results available to the community, in citable form, before we publish the edited article. This *Accepted Manuscript* will be replaced by the edited, formatted and paginated article as soon as this is available.

You can find more information about *Accepted Manuscripts* in the [Information for Authors](#).

Please note that technical editing may introduce minor changes to the text and/or graphics, which may alter content. The journal's standard [Terms & Conditions](#) and the [Ethical guidelines](#) still apply. In no event shall the Royal Society of Chemistry be held responsible for any errors or omissions in this *Accepted Manuscript* or any consequences arising from the use of any information it contains.

# Biobased copolyesters from renewable resources: Synthesis and crystallization behavior of poly(decamethylene sebacate-*co*-isosorbide sebacate)

Zhiyong Wei, Cheng Zhou, Yang Yu, Yang Li\*

*State Key Laboratory of Fine Chemicals, Department of Polymer Science and Materials, School of Chemical Engineering, Dalian University of Technology, Dalian 116024, China*

## Abstract

A series of long chain aliphatic copolyesters poly(decamethylene sebacate-*co*-isosorbide sebacate) (P(DS-*co*-IS)) were synthesized from commercially available biobased sebacic acid (SA), 1,10-decanediol (DD) and isosorbide (ISB) through a two-step melt polycondensation method. The molecular weight, composition, and microstructure of the P(DS-*co*-IS) copolyesters were characterized by GPC, <sup>1</sup>H-, <sup>13</sup>C-NMR. Crystallization properties of the P(DS-*co*-IS) copolyesters are depressed while the glass transition temperature is enhanced by the incorporation of isosorbide with bulky rigid structure. Nonisothermal melt crystallization peak temperature and melting point decrease for P(DS-*co*-IS) with increasing the ISB unit; Moreover, the equilibrium melting point temperature of P(DS-*co*-IS) is also reduced. However, the introduction of ISB segment does not change the crystal structure of P(DS-*co*-IS), but decreases gradually the crystallinity. Isothermal crystallization kinetics of neat PDS and its copolyesters indicated that PDS possesses high crystallization ability characteristics of long chain aliphatic polyester. The crystallization mechanism remains unchanged for either neat PDS and P(DS-*co*-IS), however, the crystallization rates of P(DS-*co*-IS) decrease with increasing ISB composition and crystallization temperature. No evidence of ring-banded spherulites could be detected for this long chain PDS and its copolyesters in a wide temperature range even when very low supercoolings.

**Keywords:** Biobased polyesters, long chain aliphatic polyesters, crystallization

---

\* Corresponding author.

*E-mail address:* liyang@dlut.edu.cn (Y. Li)

## 1. Introduction

Current environmental concerns, waste accumulation and disposal, as well as the inevitable depletion of fossil resources bring an increasingly interest in biobased polymers derived from renewable resources[1-2]. Nowadays, utilization of renewable molecules derived from biomass and development of environment-friendly polymers are probably two of the greatest challenges in chemical industry[3]. Therefore, the development of sustainable polymers based on naturally occurring molecules or derivative chemicals is an effective method for solving environmental problems inherent to polymer chemistry[4].

Among these biobased polymers, aliphatic polyesters undoubtedly represent one of the most promising classes, as they can be prepared from renewable resources and can be biodegraded into feedstocks with low environmental impact[5-6]. Due to their biocompatibility and biodegradability, aliphatic polyesters are attracting considerable attention from the viewpoint of environmental protection, resource recycling, and applications in many fields[7]. However, most researches focus on short chain aliphatic polyesters, such as poly(butylene succinate), poly(ethylene succinate)[8-12]. Recently, long chain aliphatic polyesters have been receiving more attention due to its unique chain characteristic [13-20]. It is interesting that the incorporation of long methylene sequences enhances polymer crystallization and renders polyesters hydrophobic. Studies showed that long chain aliphatic polyesters have relatively high crystallization and melting temperatures, suitable for thermoplastic processing, which differ from shorter chain analogs[21-22].

Some emerging biobased diacid and/or diol monomers are used for synthesis of long chain aliphatic polyesters[15-17, 23, 24]. Sebacic acid (SA), one of naturally occurring dicarboxylic acids, is an intermediate product of  $\omega$ -oxidation of long chain aliphatic acids[25]. Compared with short chain diacids, sebacic acid is more suitable for the preparation of aliphatic polyesters, as short chain analogs always tend to intramolecular condensation. Specifically, sebacic acid is a derivative of castor oil by alkali fission, which has a vast majority of world production occurring in China annually exports over 100,000 metric tonnes, representing over 90% of global trade of the product[26-27]. Meanwhile, sebacic acid can be converted into 1,10-decanediol via esterification and hydrogenation processes. Therefore, the availability of large-scale products of both sebacic acid and 1,10-decanediol makes them to be potential renewable resources for biobased polyesters. Although many sebacic acid based polyesters have been synthesized for biomedical applications [28-35], however, there is still no attempt to long chain aliphatic polyester derived from sebacic acid and 1,10-decanediol. Moreover, the poly(decamethylene sebacate) (PDS) has a  $-(CH_2)-$  sequence long enough to give some interesting new properties and to suggest some structure-properties correlations.

Unfortunately, the thermal properties and durability of PDS is unsatisfactory in some applications like other aliphatic polyesters. An efficient strategy to enhance the performances of this type of material is to introduce some rigid

molecular structure into polymeric backbone[36]. Isosorbide (1,4:3,6-dianhydro-D-glucitol, ISB) with rigid molecular structure and chirality is an ideal candidate that can satisfy above issues [37]. Meanwhile, isosorbide is a renewable monomer derived from glucose by a fermentation process, which is also the only bicyclic carbohydrate-based monomer commercially available at an industrial level[38]. Although it has been extensively used to improve the thermal stability and glass transition temperature of polyesters[39-48], the relationships between structure and properties are not well-established for long chain aliphatic polyesters with incorporation of isosorbide.

In this work, we firstly synthesized a series of biobased copolyesters poly(decamethylene sebacate-*co*-isosorbide sebacate) (P(DS-*co*-IS)) based on sebacic acid in combination with 1,10-decanediol and isosorbide. Since the physical properties and biodegradability of biodegradable polymers are greatly dependent on the spherulite morphology, crystal structure and degree of crystallinity[49], it is of great importance to investigate the crystallization and morphology behavior of long chain aliphatic polyesters. Meanwhile, the effect of the bulky rigid molecular structure of isosorbide on microstructure and thermal properties of the copolyesters was also emphasized. It is expected that the results presented herein will be of help for a better understanding of the structure-property relationships in the case of long chain aliphatic copolyesters.

## 2. Experimental

### *Materials*

Sebacic acid (SA, 99%), 1,10-decanediol (DD, 98.5%), Isosorbide (ISB, 98%), and stannous octoate ( $\text{Sn}(\text{Oct})_2$ , >96%), were purchased from J&K Chemical. All other reagents were used as received.

### *Synthesis of copolyesters*

The P(DS-*co*-IS) copolyesters were synthesized by a two-step esterification and polycondensation process, as depicted in Scheme 1. The molar ratio of SA/(DD+ISB) was 1.05/1, appropriate amount of  $\text{Sn}(\text{Oct})_2$  was used as catalyst. During the first stage, the mixture was heated to 180°C and reacted 3~4 h under nitrogen atmosphere to complete the esterification process. In the polycondensation step, the pressure was reduced to 100 Pa and the temperature was raised up to 230 °C to remove completely the byproduct and the unreacted monomers, and the polycondensation was continued for 2~3 h. The resulting copolyesters were dissolved in chloroform and precipitated with ethanol twice, then dried at 20 °C under vacuum for 24h. Homopolymers poly(decamethylene sebacate) (PDS) and poly(isosorbide sebacate) (PIS) were also prepared by similar synthetic procedure for comparison. The samples with various feed ratios are listed in Table 1.

### *Characterization*

The molecular weight and its distribution were measured by gel permeation chromatography (GPC) using a Waters 1515 HPLC system equipped with Ultrastaygel® columns and differential refractometer detector. Tetrahydrofuran (THF) was used as the eluent at a flow rate of 1.0 mL/min at 25 °C. The molecular weights were calculated from the polystyrene standards with narrow polydispersity.

<sup>1</sup>H NMR spectra were performed on Bruker Avance 400MHz spectrometer at a 400 MHz resonance frequency with 32 scans, a 4.0 s acquisition time and a 6.5 ms pulse width. <sup>13</sup>C NMR spectra were recorded at a resonance frequency of 100 MHz with 17,000 scans, a 1.4 s acquisition time and a 6.5 ms pulse width. Deuterated chloroform (CHCl<sub>3</sub>) and tetramethylsilane (TMS) were used as the solvent and the calibration, respectively.

Differential scanning calorimetry (DSC) was carried out on DSC1 (Mettler Toledo, Switzerland) instrument under nitrogen atmosphere. The samples were heated for the first run from 25 to 130 °C for 5 min to erase thermal history, then cooled to -70 °C at a rate of 10 °C/min, and heated again for the second run from -70 to 130 °C at a rate of 10 °C/min. The crystallization peak temperature ( $T_c$ ) and its entropy ( $\Delta H_c$ ) were obtained from the DSC cooling run. The glass transition temperature ( $T_g$ ), melting temperature ( $T_m$ ) and entropy of fusion ( $\Delta H_m$ ) were measured on the second heating scanning. For the investigation of isothermal crystallization kinetics, the samples were initially melted at 130 °C for 3 min then quenched to the desired crystallization temperature at a rate of 60 °C/min. After the completion of isothermal crystallization, the samples were directly heated to the melt at a rate of 10 °C/min. The heat flows during both crystallization and melting processes were recorded for the later kinetics analysis of isothermal crystallization and the estimation of the equilibrium melting point.

Wide-angle X-ray diffraction (WAXD) experiments were performed on a Dmax-Ultima + X-ray diffractometer with Ni-filtered Cu/K $\alpha$  radiation ( $\lambda=0.15418$  nm). The operating target voltage was 40KV and the tube current was 100 mA. The scanning speed was 1.2°/min from 10° to 30°. The films (ca. 1 mm thickness) for WAXD measurements were hot-pressed and followed by cooling to room temperature.

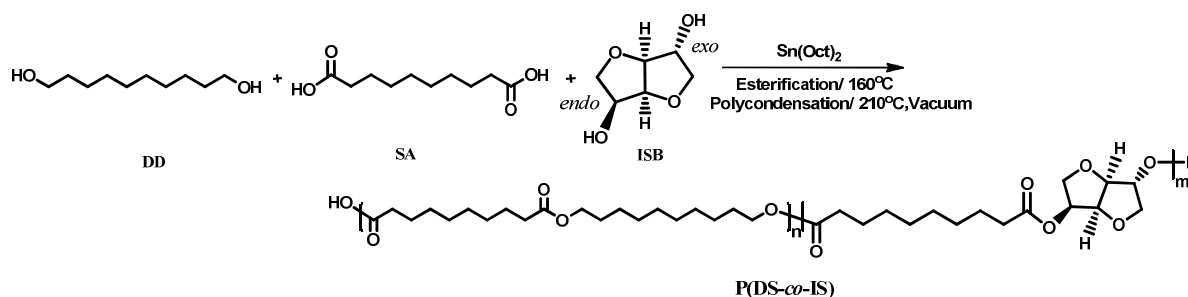
Spherulite morphologies of the copolyesters were observed by a Leica DM4500P polarized optical microscope (POM) equipped with a Linkam THMS600 hot stage. The samples were placed between two cover glasses, melted and pressed at 120 °C for 3min, then quenched to predetermined temperature ( $T_c$ ) for isothermal crystallization, and the representative spherulitic morphologies were recorded.

### 3. Results and discussion

#### 3.1 Synthesis and characterization of copolyesters

Biobased copolyesters poly(decamethylene sebacate-*co*-isosorbide sebacate) (P(DS-*co*-IS)) were synthesized by a traditional two-step melt esterification and polycondensation process, as shown in **Scheme 1**. The molecular

characteristics of the copolyesters obtained by GPC are listed in **Table 1**. At the low content of ISB (<30%), the number average molecular weight ( $M_n$ ) ranging from 11300 to 17000 g/mol and weight average molecular weight ( $M_w$ ) ranging from 18100 to 29400 g/mol are obtained with dispersity index ( $\mathcal{D}$ ) from 1.59 to 1.73, as expected for this synthetic method used [50]. With increasing ISB contents (>30%), the number average molecular weights of the copolyesters significantly decrease, and  $M_n$  of homopolymer poly(isosorbide sebacate) is lower than 3000. The depression of the molecular weights of the isosorbide based copolyesters results from its low reactivity [38]. On one hand, the secondary alcohol moieties of isosorbide present a lower reactivity with respect to primary alcohol, mainly due to a corresponding lower acidic character, and on the other hand, the steric hindrance of the *endo* hydroxyl group of ISB further decreases the reactivity of the system [41].



**Scheme 1** Synthetic route of poly(decamethylene sebacate-*co*-isosorbide sebacate) (P(DS-*co*-IS)) copolyesters

**Table 1** Composition and molecular weight of P(DS-*co*-IS) copolyesters

Sample	DD/ISB in feed (molar ratio)	DD/ISB in copolymer <sup>a</sup> (molar ratio)	$M_n$ (Da) <sup>b</sup>	$M_w$ (Da) <sup>b</sup>	$\mathcal{D}^b$
PDS	100/0	100/0	17600	28000	1.59
P(DS- <i>co</i> -5.3mol% IS)	90/10	94.7/5.3	15300	24000	1.57
P(DS- <i>co</i> -16.7mol% IS)	80/20	83.3/16.7	14300	24300	1.70
P(DS- <i>co</i> -25.4mol% IS)	70/30	74.6/25.4	17000	29400	1.73
P(DS- <i>co</i> -43.9mol% IS)	50/50	56.1/43.9	8900	14300	1.61
P(DS- <i>co</i> -66.2mol% IS)	30/70	33.8/66.2	8600	13800	1.61
PIS	0/100	0/100	2800	5300	1.89

<sup>a</sup> Calculated by integration of  $^1\text{H}$  NMR spectra;

<sup>b</sup> Measured by GPC in THF against PS

The chemical structure and composition of the P(DS-*co*-IS) copolyesters were evaluated by using  $^1\text{H}$  NMR spectroscopy. Firstly, the  $^1\text{H}$  NMR spectra of two homopolymers poly(decamethylene sebacate) (PDS) and poly(isosorbide sebacate) (PIS) were presented in **Fig. 1**. The  $^1\text{H}$  NMR spectrum of PDS is very simple, and its four characteristic peaks are easily assigned and showed in **Fig. 1 (a)**. In the case of PIS, six signals (Numbers 1-6) in the range between 4.6 ppm and 5.4 ppm are attributed to the eight protons of isosorbide (ISB), and the assignments are

highlighted in **Fig. 1(b)**. It is interesting to observe that the signals of the methylene linked to carbonyl in sebacate unit split into two equal groups ( $f_1$  and  $f_2$ ), which are caused by the chemical difference between *exo* and *endo* linked hydroxyl groups in isosorbide unit.

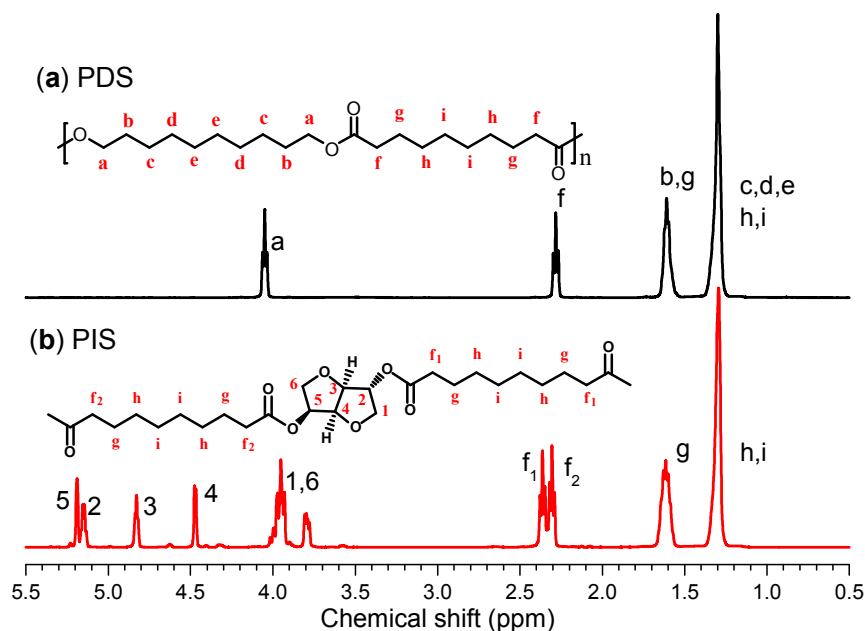


**Fig. 1**  $^1\text{H}$ -NMR spectra of homopolymers: (a) poly(decamethylene sebacate) and (b) poly(isosorbide sebacate)

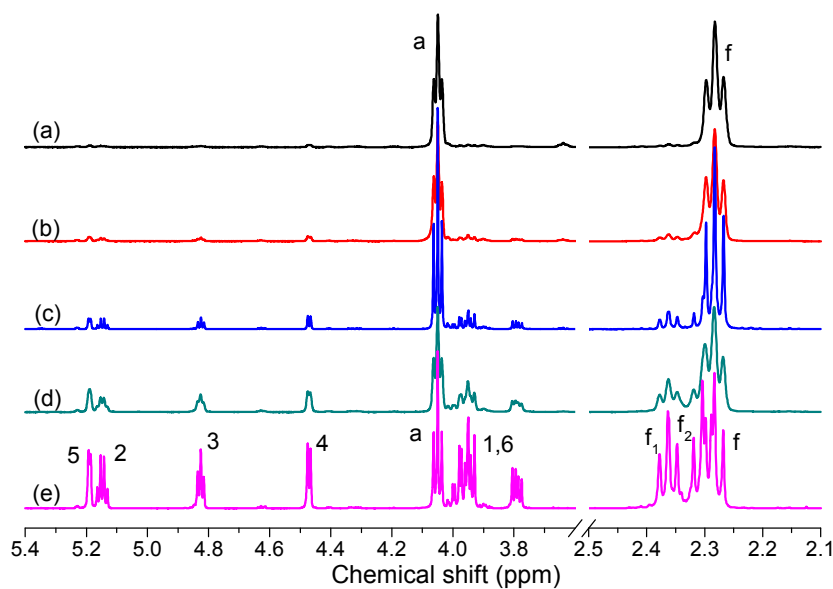


**Fig. 2** Enlarged  $^1\text{H}$ -NMR spectra of P(DS-co-IS) copolyesters for calculation of composition: (a) P(DS-co-5.3mol% IS), (b) P(DS-co-16.7mol% IS), (c) P(DS-co-25.4mol% IS), (d) P(DS-co-43.9mol% IS), and (e) P(DS-co-66.2mol% IS).

Observed from down to up in **Fig. 2** of the  $^1\text{H}$  NMR spectra of the P(DS-co-IS) copolyesters, the characteristic peaks of 1,10-decanediol (DD) decrease and the characteristic peaks of isosorbide (ISB) increase, which are subject to the feed ratios. The molar ratio of DD to ISB is calculated from the integration areas of these protons peaks of each diol

in **Fig. 2** of the  $^1\text{H}$  NMR spectra, and the results are summarized in **Table 1**. It can be found that the calculated relative content of ISB in copolymer is obviously lower than that in the monomer feed ratio. Similar to other report on copolymerization of isosorbide with aliphatic diols [44], such losses can be attributed to the lower reactivity of the secondary hydroxyl groups of ISB than that of the primary hydroxyl groups of DD.

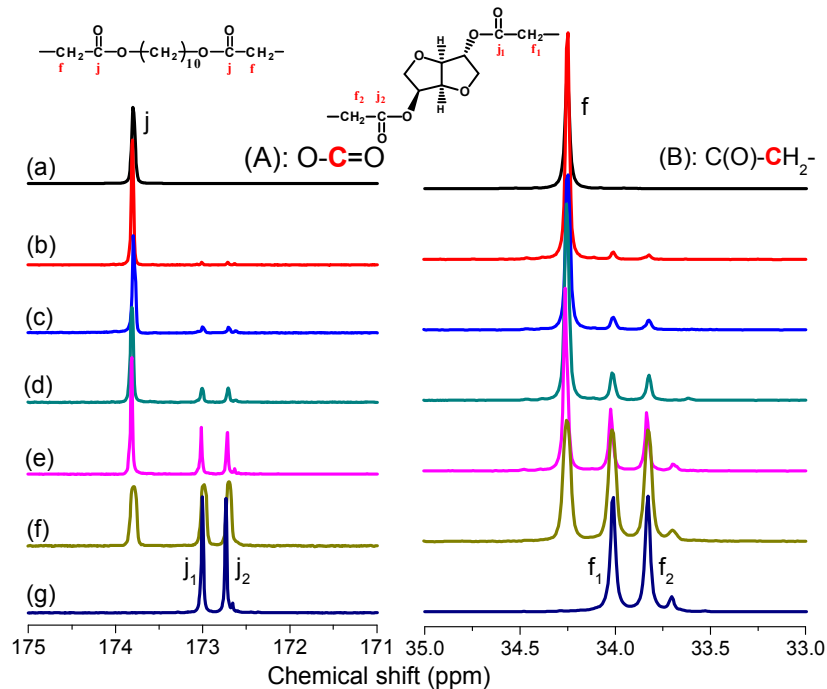


**Fig. 3** (A): Carbonyl region and (B) Methylene region in  $^{13}\text{C}$ -NMR spectra of P(DS-co-IS) copolyesters: (a) PDS, (b) P(DS-co-5.3mol% IS), (c) P(DS-co-16.7mol% IS), (d) P(DS-co-25.4mol% IS), (e) P(DS-co-43.9mol% IS), (f) P(DS-co-66.2mol% IS), (g) PIS.

$^{13}\text{C}$  NMR is a powerful tool to analyze the chain microstructure of copolymers, since it is sensitive to monomer sequence. In particular, the carbonyl signal is very sensitive to the neighboring diol units, consequently, its splitting has been reported for short chain aliphatic copolyesters [51-52]. Therefore, it is commonly used to analyze the random copolyesters and determine the sequence length of each comonomer, which is one of the key parameters determining the physical properties of copolymers. **Fig. 3(A)** shows the carbonyl signals in  $^{13}\text{C}$  NMR of the homopolyesters and their copolyesters. In contrast to that one single peak ( $j$ ) is observed for PDS, two equal peaks ( $j_1$  and  $j_2$ ) are found for PIS, which are assigned to the carbonyl carbon linked the *exo* and *endo* hydroxyl groups of ISB, respectively. It resembles the previous phenomenon of proton signals ( $f_1$  and  $f_2$ ) of the terminal methylene of sebacate unit. Unfortunately, the carbonyl peaks of the copolyesters are only composed of the signals of two parent polyesters, no new splitting peak between them is detectable. The same results are observed for the carbon signals of the methylene linked to carbonyl in sebacate segment from **Fig. 3(B)**. The results suggest that the carbon signals in sebacic acid based

copolyesters are insensitive to a triad effect. Therefore, no information concerning sequence distribution could be derived for P(DS-*co*-IS) copolyesters. It is reasonably attributed to the shielding effect of long methylene sequences in long chain aliphatic sebacate. For the time being, there is no clear explanation for this fact, and further structural studies are required. Nevertheless, random copolyesters are expected to obtain due to the random condensation reaction and transesterification during the preparation process [50]. We hypothesize that the sequence distribution of the copolyesters in this study is random [53], which is evidenced by the depressed melting point demonstrated in the following context.

### 3.2 Nonisothermal analysis: crystallization and melting behavior

Standard DSC was carried out to measure the basic thermal properties of the P(DS-*co*-IS) copolyesters by thermal cycles. **Fig. 4(A)** shows the DSC cooling traces of nonisothermal melt crystallization at cooling rate of 10 °C/min. It is found that the crystallization exotherms of PDS and its copolyesters with incorporation of low ISB contents are very narrow and sharp, and the crystallization peak temperature ( $T_c$ ) of the copolyesters shifts to lower temperature and the corresponding  $\Delta H_c$  decreases with increasing ISB content. These curves are typical of long chain aliphatic polyesters with high tendency to crystallize into perfect and stable crystals. Even that the P(DS-*co*-66.9mol% IS) with only 33.1mol% DS units also occurs melt crystallization, although its crystallization ability has been significantly depressed by the large steric hindrance of asymmetric bicyclic structure of ISB. Also the crystallization enthalpy ( $\Delta H_c$ ) tends to be reduced with respect to PDS, as reported in **Table 2**. In regards to homopolymer PIS, however, the crystallization exotherm finally disappears, suggesting that PIS totally loses the crystallizability due to the presence of 100% ISB with rigid structure, evidenced by the fact that it cannot crystallize even at very slow cooling rate (not shown here).

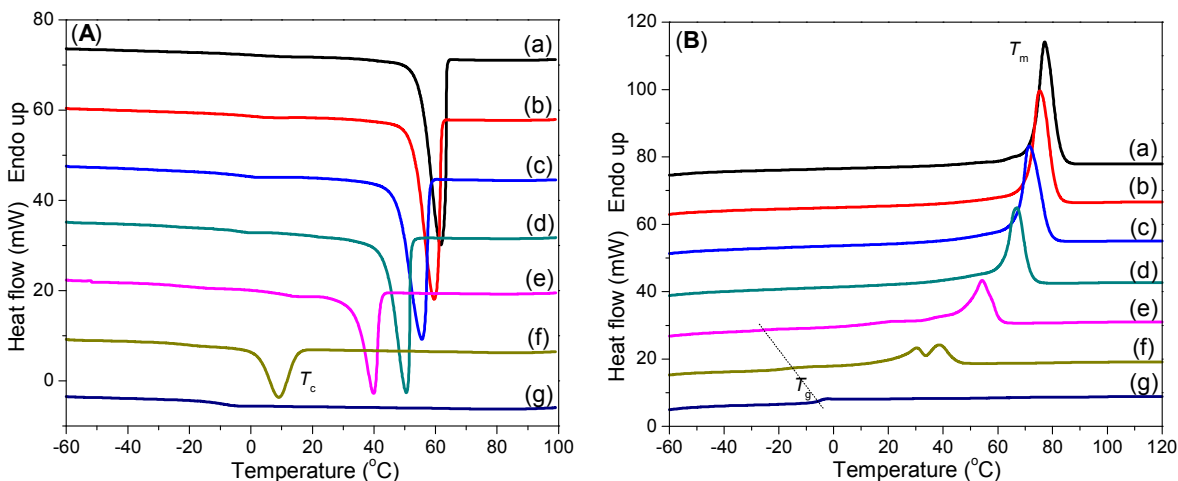


**Fig. 4** DSC recorded at 10K/min (A) cooling and (B) 2nd heating curves of P(DS-*co*-IS) copolyesters: (a) PDS, (b) P(DS-*co*-5.3mol% IS), (c) P(DS-*co*-16.7mol% IS), (d) P(DS-*co*-25.4mol% IS), (e) P(DS-*co*-44.4mol% IS), (f) P(DS-*co*-66.9mol% IS), (g) PIS

**Table 2** Thermal parameters of the P(DS-co-IS) copolyesters

Sample	$T_g(^{\circ}\text{C})$	$T_c(^{\circ}\text{C})$	$\Delta H_c(\text{J/g})$	$T_m(^{\circ}\text{C})$	$\Delta H_m(\text{J/g})$
PDS	n.a. <sup>a</sup>	62.3	125.4	75.8	128.7
P(DS-co-5.3mol% IS)	n.a.	60.2	104.1	74.1	103.3
P(DS-co-16.7mol% IS)	n.a.	55.6	98.4	71.4	100.5
P(DS-co-25.4mol% IS)	n.a.	50.5	77.3	66.9	78.0
P(DS-co-43.9mol% IS)	-26	39.9	47.4	54.2	49.6
P(DS-co-66.2mol% IS)	-18	9.1	31.9	30.4, 38.5	37.2
PIS	-5	n.a.	n.a.	n.a.	n.a.

<sup>a</sup>: not available.

The subsequent melting curves of the copolyesters are presented in **Fig. 4(B)**. For PDS and its copolyesters with low ISB contents a rather single melting endotherm is observed. It indicates that the resultant crystals are considerable perfect and stable, accordingly, they melt directly without undergoing reorganization and recrystallization. This is different from the multiple melting behaviors commonly observed for short chain aliphatic polyesters[8-12]. This difference can be attributed to the faster crystallization rate of long chain aliphatic polyesters, thanks to the higher flexibility of the chain with long  $-(\text{CH}_2)-$  sequences[22]. The melting temperature ( $T_m$ ) and the corresponding fusion enthalpy ( $\Delta H_m$ ) are depressed significantly with increasing ISB content, which are consistent with the trend of  $T_c$  and  $\Delta H_c$ .

Unfortunately, no remarkable glass transition is detected for PDS and its copolyesters with ISB lower than 30%. As previously discussed, long chain aliphatic polyesters have strong crystallization capacity and crystallize very fast, and crystallization could not be depressed even by quenching[49]. Nevertheless, a single glass transition is observed for the P(DS-co-IS) copolyesters when the content of ISB is higher than 40%, especially in the case of PIS with 100% ISB. The finding that only a single  $T_g$  can be detectable also supports that the P(DS-co-IS) copolyesters are hypothesized to being random copolyesters. In addition, the incorporation of ISB into copolymeric chains enhances its glass transition temperature. This trend is attributed to decrement in the chain flexibility, which is caused by the large steric hindrance of ISB.

### 3.3 Isothermal crystallization behavior

To further obtain detailed crystallization information, isothermal crystallization kinetics of PDS and its three copolyesters with ISB lower than 30% was investigated by differential scanning calorimetry (DSC) at different temperature intervals. **Fig. 5** represents a series of well-normal bell-shaped exotherms of PDS and its copolyesters during isothermal crystallization process. For the sake of the completion of crystallization within an approximate

crystallization time, the intervals of crystallization temperature of the copolyesters gradually shift to lower temperature ranges than that of PDS. This shift reveals that the crystallization rate of the copolyesters is reduced greatly by the incorporation of ISB into the polymeric chains. It is evident that the bulky and asymmetric structure of bicycle ISB disrupts the chain regularity and restricts the chain mobility, consequently, leading to the depression of polymer crystallization. Meanwhile, it is observed that for each sample, as the isothermal crystallization temperature ( $T_c$ ) increases, the exothermic peak becomes broader and shifts to a longer crystallization time. As expected, with increasing crystallization temperature, the crystallization rate of the copolyesters decreases and it requires a longer time to achieve the completion of crystallization.

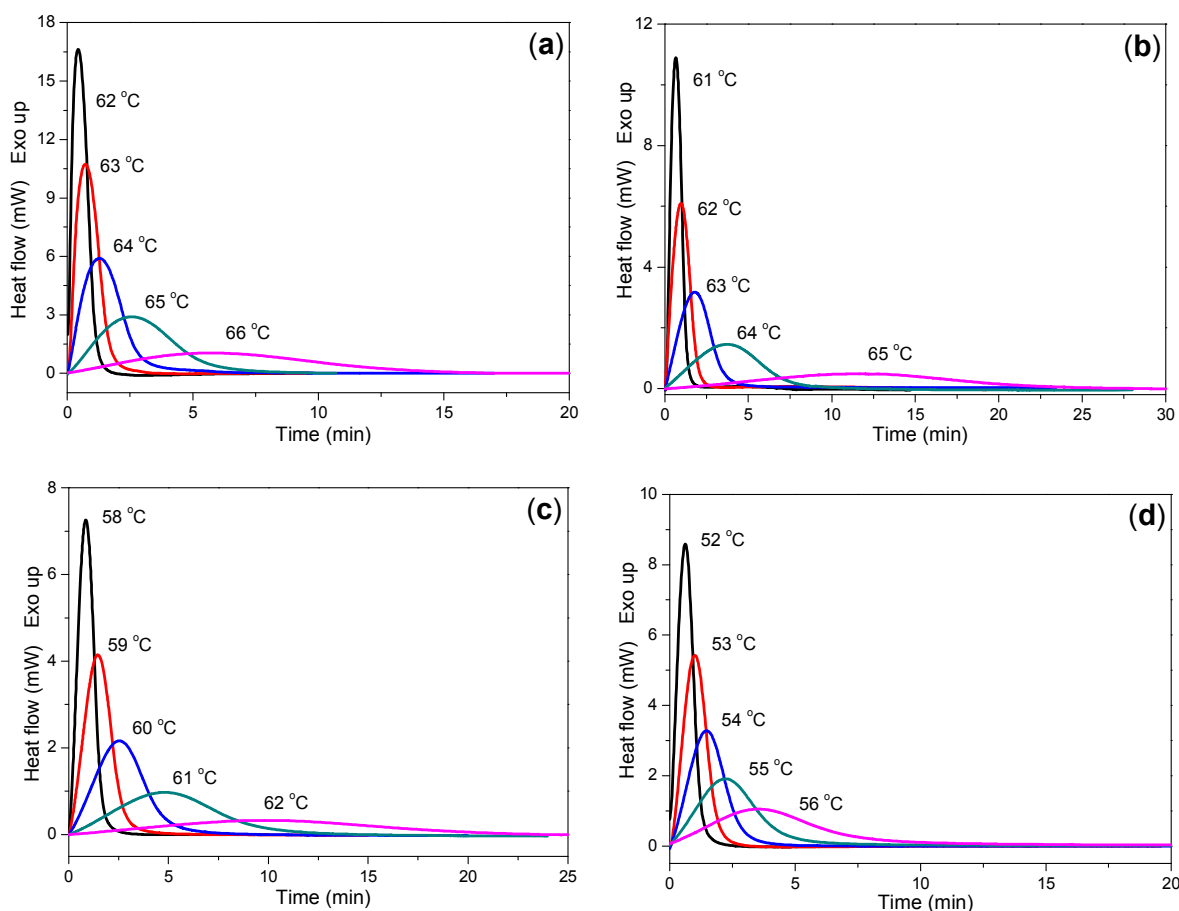


**Fig. 5** DSC thermograms of P(DS-co-IS) copolyesters for isothermal crystallization at different temperatures: (a) PDS, (b) P(DS-co-5.3mol% IS), (c) P(DS-co-16.7mol% IS), (d) P(DS-co-25.4mol% IS)

With the purpose of understanding the isothermal crystallization process, a comparative study of the crystallization kinetics of neat PDS and its copolyesters is carried out. Based on the assumption that the evolution of crystallinity is linearly proportional to the evolution of heat released during the crystallization, the relative degree of crystallinity,  $X_t$ , can be calculated by integration of the exothermic peaks according to the following equation:

$$X_t = \frac{X_t(t)}{X_t(\infty)} = \frac{\int_0^t (dH_c / dt) dt}{\int_0^\infty (dH_c / dt) dt} \quad (1)$$

where  $dH_c/dt$  denotes the rate of heat flow,  $X_t(t)$  and  $X_t(\infty)$  represent the absolute crystallinity at the elapsed time during the course of crystallization and at the end of the crystallization process, respectively.

The evolution of relative crystallinity with crystallization time at various temperatures (PDS as an example shown in **Fig.6(a)**) shows the similar S-shaped curves, which are consistent with nucleation and growth processes. The half time of crystallization at 50% relative crystallinity ( $t_{1/2}$ ) obtained from these curves is frequently used to evaluate the crystallization rate of PDS. The obtained  $t_{1/2}$  values for the samples are summarized in **Table 3**. It is obvious that  $t_{1/2}$  is an important parameter for the evaluation of crystallization kinetics. The crystallization rate can thus be easily described by the reciprocal of  $t_{1/2}$ . As expected, the values of  $t_{1/2}$  increase with increasing  $T_c$  for all the samples, indicating that the crystallization rate decreases with increasing  $T_c$ . Accordingly, the values of  $1/t_{1/2}$  for the copolyesters are much smaller than that of PDS at a given  $T_c$ . This indicates that the crystallization rate of the copolyesters is reduced by the incorporation of ISB with specific bulky structure, as previously discussed.

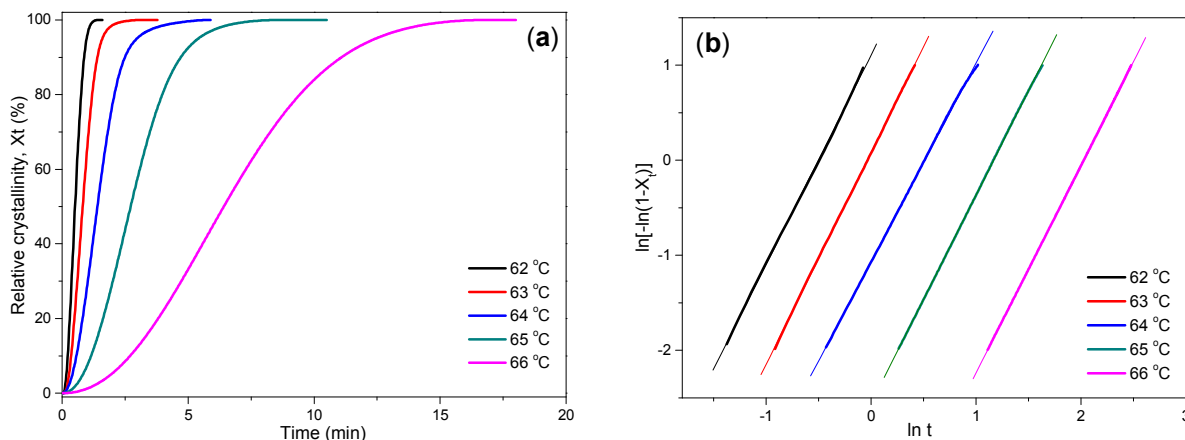


**Fig. 6** (a) Relative degree of crystallinity with time and (b) Avrami plots of  $\ln[-\ln(1-X_t)]$  versus  $\ln t$  of PDS for isothermal crystallization at different temperatures

Furthermore, the evolution of crystallinity during the isothermal crystallization process was analyzed by the widely used Avrami model [54]. Accordingly, the relative degree of crystallinity,  $X_t$ , is related to the crystallization time,  $t$ , can be expressed as,

$$X_t = 1 - \exp(-kt^n) \quad (2)$$

$$\ln[-\ln(1-X_t)] = \ln k + n \ln t \quad (3)$$

where  $n$  is the Avrami exponent, which is relevant to the mechanism of nucleation, and it contains information on nucleation and growth geometry, and  $k$  is the overall crystallization rate constant, which is dependent on nucleation and crystal growth.

The representative Avrami plots for PDS obtained at various temperatures are illustrated in **Fig. 6(b)**. It is important to note that the linearity in the plots, which corresponds to a degree of crystallinity in a wide relative crystallinity range, is very satisfactory. From the slope and the intercept of the Avrami plots, the parameters  $k$  and  $n$ , respectively, are estimated and summarized in **Table 3**. For each sample, the crystallization rate constant  $k$  decreases as the crystallization temperature increases. Meanwhile, the  $k$  values of the copolyesters are smaller than that of PDS at a given crystallization temperature. This also suggests that the crystallization process of the copolyesters is retarded with increasing the ISB contents, which is in accordance with the aforementioned results. As can be observed from **Table 3**, the average values of  $n$  for all samples are in the range between 2.2 and 2.5, which suggesting that both two- and three-dimensional crystal growths simultaneously occur [55]. The slight variation of  $n$  also indicates that the mechanism of nucleation and the manner of crystal growth of the copolyesters has not been greatly altered by the incorporation of ISB units into PDS chains.

**Table 3** Avrami analysis for isothermal crystallization of P(DS-*co*-IS) copolyesters

Sample	$T_c(^{\circ}\text{C})$	$t_{1/2}(\text{min})$	$K(\text{min}^{-n})$	$n$	$n(\text{average})$
PDS	62	0.50	3.004	2.20	2.2
	63	0.82	1.083	2.23	
	64	1.40	0.343	2.09	
	65	2.72	0.077	2.19	
	66	6.42	0.012	2.18	
	P(DS- <i>co</i> -5.3mol% IS)	61	0.68	1.870	
62		0.98	0.733	2.32	
63		1.82	0.174	2.36	
64		3.72	0.032	2.36	
65		11.90	0.002	2.46	
P(DS- <i>co</i> -16.7mol% IS)	58	0.88	0.970	2.57	2.5
	59	1.48	0.254	2.54	
	60	2.62	0.066	2.43	
	61	5.04	0.015	2.37	
	62	10.28	0.003	2.38	
P(DS- <i>co</i> -25.4mol% IS)	52	0.64	2.219	2.59	2.4
	53	0.93	0.850	2.52	
	54	1.48	0.273	2.41	
	55	2.38	0.093	2.28	
	56	3.90	0.034	2.21	

### 3.4 Equilibrium melting point

The equilibrium melting point ( $T_m^0$ ) is an important parameter for evaluating thermodynamics of crystallization. In fact it is impossible to obtain the final thermodynamically stable polymer lamellar crystal in experiment due to the kinetic factors. Moreover, it is well known that  $T_m^0$  depends not only the kinetic factors such as metastability of chain-folded crystals and the experimental conditions such as heating rate of DSC scanning, but also the extrapolation method used. Thus,  $T_m^0$  is generally extrapolated from the observed melting temperature ( $T_m$ ). Hoffman-Weeks method has been widely used to determine the equilibrium melting temperature because of the experimental and analytical simplicities. According to Hoffman-Weeks theory[56],  $T_m^0$  can be easily obtained from the following equation:

$$T_m = \frac{T_c}{\gamma} + \left(1 - \frac{1}{\gamma}\right) T_m^0 \quad (4)$$

where  $\gamma$  is the thickening coefficient, which depends on the lamellar thickness during the crystallization.

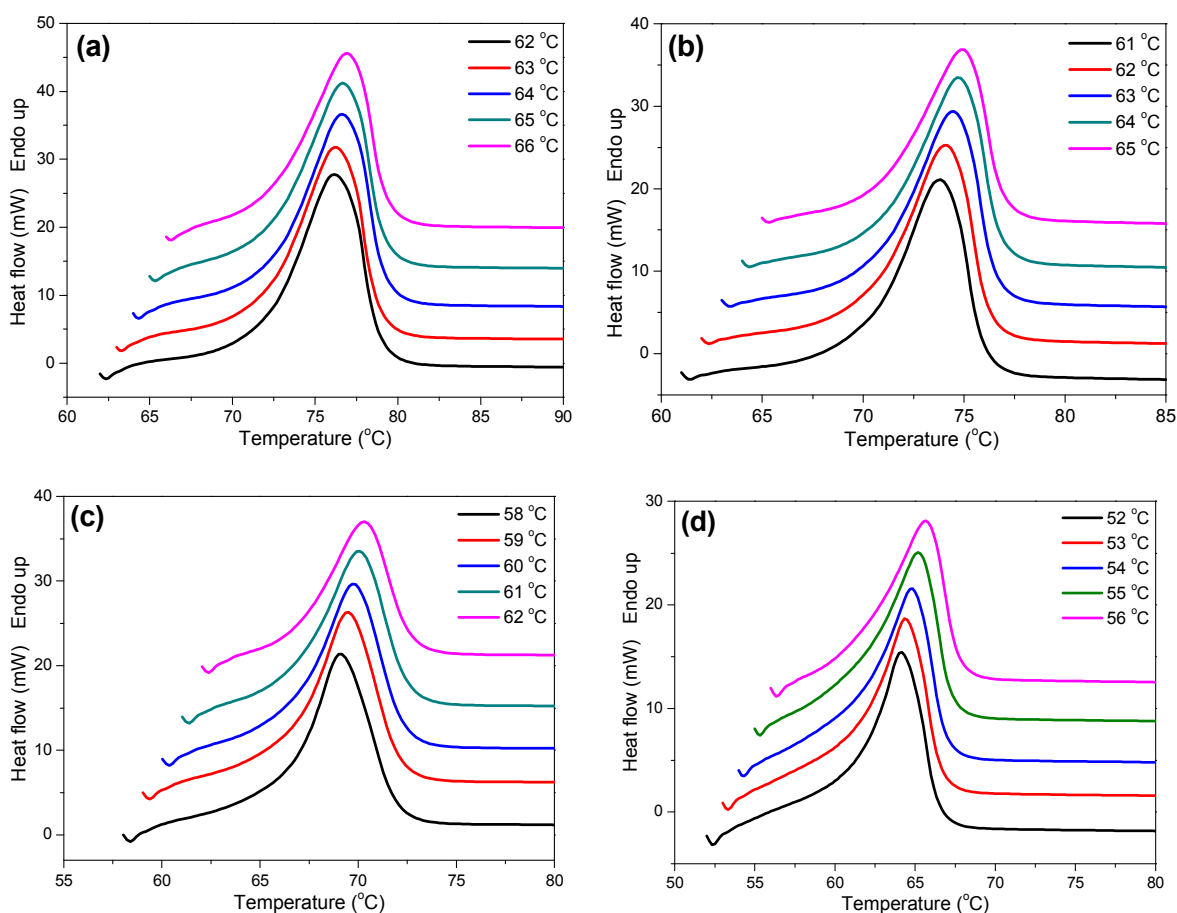


**Fig. 7** Melting behaviors of (a) PDS, (b) P(DS-co-5.3mol% IS), (c) P(DS-co-16.7mol% IS), (d) P(DS-co-25.4mol% IS) after isothermal crystallization at different temperatures

According to this equation,  $T_m^0$  can be obtained simply from the intersection of the  $T_m = T_c$  line, by using the DSC method to measure the observed melting temperature ( $T_m$ ) at different crystallization temperature ( $T_c$ ). Thus, the

subsequent melting behavior of PDS and its three copolyesters was recorded by DSC after the completion of isothermal crystallization. As shown in **Fig. 7**, a rather single melting endotherm is found for all the samples within the tested  $T_c$  range, due to the formation of more perfect and stable crystals during isothermal crystallization process. Interestingly, it is different from the multiple melting phenomena observed commonly for short chain aliphatic polyesters, whose imperfect and less stable crystals formed in isothermal crystallization process will undergo melt-recrystallization and reorganization into more stable crystals upon heating to the melt. It is incredible that multiple melting behavior is not observed even in the case of P(DS-co-25.4mol% IS) with considerable high ISB content. It indicates that the containing-ISB PDS chain segment still can crystallize into perfect lamellar, although the crystallization rate is reduced somewhat by the introduction of ISB-containing chain segment. Meanwhile, it also implies that the crystallization capacity of long chain aliphatic polyesters is much stronger than that of short chain analogues.

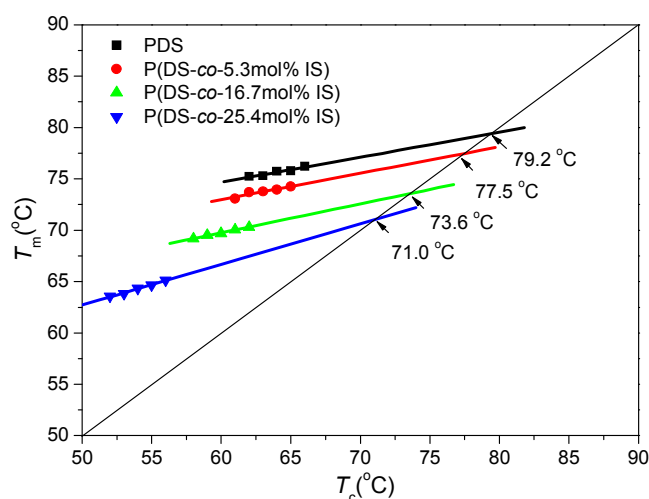


**Fig. 8** Hoffman-Weeks plots of P(DS-co-IS) copolyesters

**Fig. 8** shows the Hoffman-Weeks plots for PDS homopolymer and its three copolyesters. It is found that the values of  $T_m$  of the copolyesters are lower than that of PDS at a given  $T_c$ . As shown in **Fig.8**, the value of  $T_m^0$  is determined to be 79.2 °C for neat PDS, and those of  $T_m^0$  for the three copolyesters are determined to be from 77.5 °C to 71.0 °C with increasing ISB contents from 5.3 to 25.4 mol%. As a consequence,  $T_m^0$  of the copolyesters is induced by the incorporation of ISB with bulky structure. It is consistent with that both crystallinity and crystallization rate of the copolyesters are continuously depressed with increasing ISB content, as discussed previously. This low temperature can also be justified by considering that the rigid ISB units present along the chain are defects and distort the chain conformation and packing in the crystalline state[57]. Another effect is linked to the density of the ester groups in the polyesters which act as defects along the chain and create difficulty in folding and in reaching high crystal perfection [58]. Therefore, except for the chain flexibility, the characteristics of the crystal structure and chain conformation also have to be considered to better understand the thermal behavior.

### 3.5 Crystal structure and spherulitic morphology

In order to illustrate the relationship between the chemical composition and the crystallizability of the copolyesters, it is of great importance to investigate the crystal structure and spherulitic morphology. The crystal structures of PDS and its three copolyesters are further performed with WAXD. As shown in **Fig. 9**, two main peaks at  $2\theta \approx 21.5^\circ$  and  $24.0^\circ$  are assigned to the characteristic reflections of PDS crystal phase. No new peak is observed for the copolyesters and they show similar diffraction patterns with that of PDS. The results indicated that the introduction of ISB segment does not change the crystal structure of neat PDS, although a complete structural characterization is not reported yet. It also implied that the ISB-containing chain segment is excluded from crystal region of PDS and subject to present as an amorphous region, due to its bulky pendent group and asymmetric chemical structure. Although the locations of the diffraction peaks keep almost unchanged, the intensity of diffraction peaks decrease with the increase of the ISB content, suggesting the crystallinity of the copolyesters are depressed as compared to that of PDS. The degree of crystallinity ( $X_c$ ) can be further estimated. The values of crystallinity ( $X_c$ ) were further calculated on the basis of the WAXD patterns to be 65.1%, 59.6%, 46.7%, and 34.3% for neat PDS and its three copolyesters, respectively. The results are in accordance with previous DSC results that the fusion enthalpy ( $\Delta H_m$ ) of the copolyesters decreased with the increase of ISB contents.

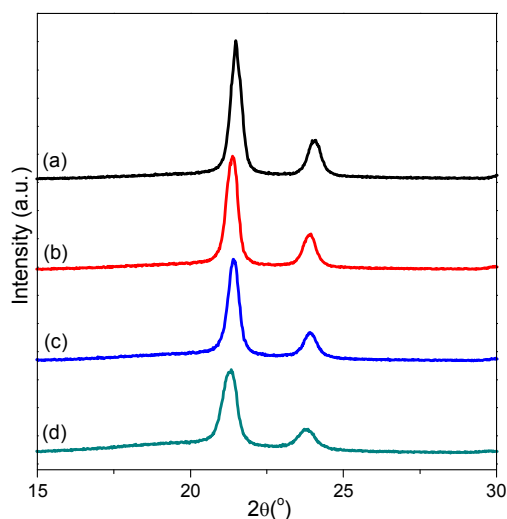


**Fig. 9** WAXD patterns of P(DS-co-IS) copolyesters: (a) PDS, (b) P(DS-co-5.3mol% IS), (c) P(DS-co-16.7mol% IS), (d) P(DS-co-25.4mol% IS)

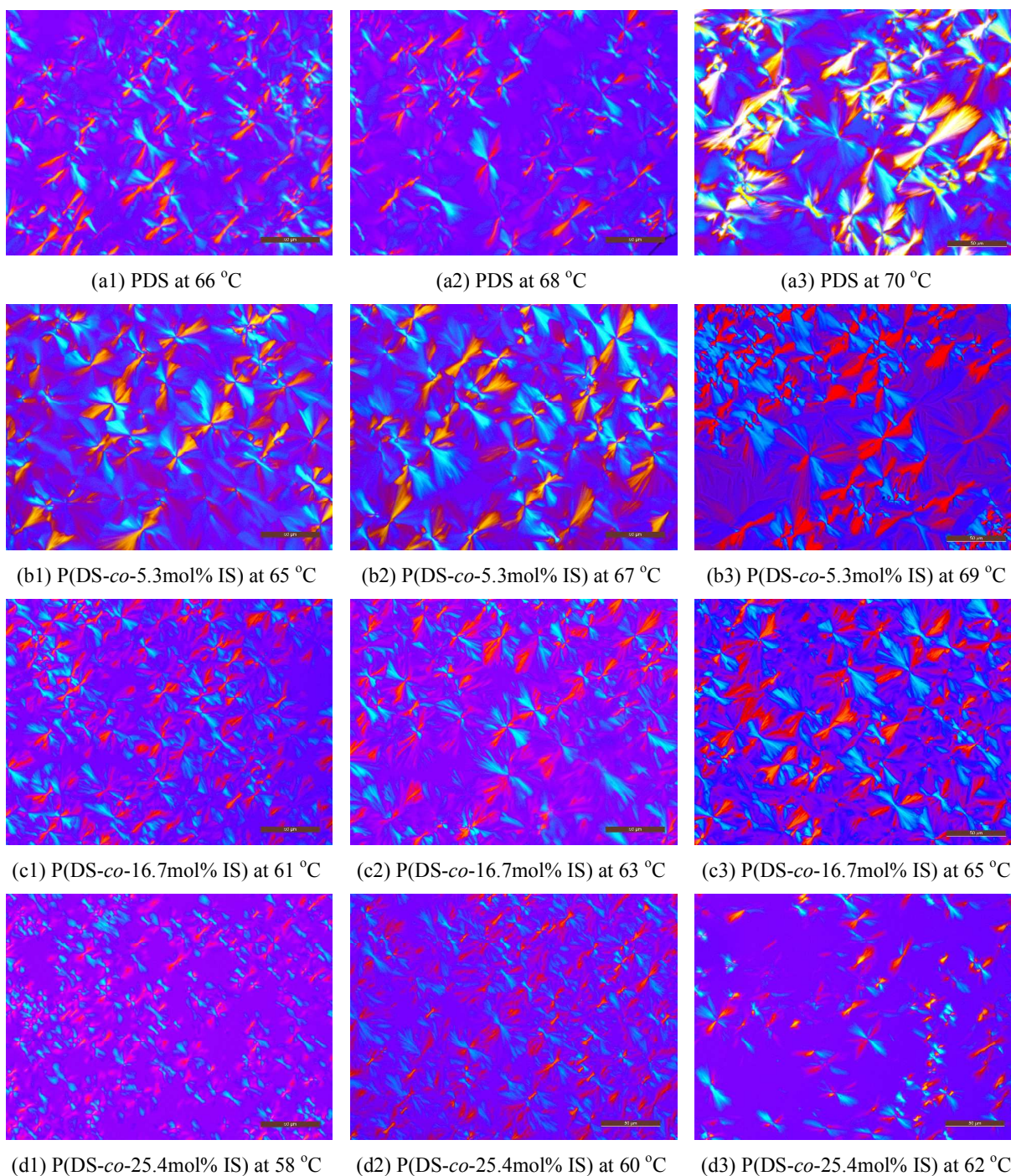


**Fig. 10** Spherulitic morphologies of (a) PDS, (b) P(DS-co-5.3mol% IS), (c) P(DS-co-16.7mol% IS), (d) P(DS-co-25.4mol% IS) after isothermal crystallization at indicated temperatures. (Scale bar=50  $\mu$ m)

It is well-known that the final physical properties and degradability are greatly dependent on the spherulitic morphology, the effects of the ISB composition and crystallization temperature on the spherulitic morphologies of neat PDS and its three copolyesters with low ISB content were further investigated by POM. **Fig. 10** displays a series of POM images of PDS and its three copolyesters isothermally crystallized at various temperatures. As a whole, with

increasing  $T_c$ , the nucleation density of each sample becomes smaller due to the difficulty of nucleation at higher  $T_c$ . Subsequently, the size of spherulites becomes larger prior to their impinging against each other. On the other hand, with the increase of ISB contents in copolymers, a trend that the nucleation density of the three copolyesters increases and their spherulitic size reduces is observed. Because PDS and its copolyesters crystallized at almost same supercooling ( $\Delta T = T_m^0 - T_c$ ), the difference of the nucleation density caused by the supercooling can be ruled out. Such increase of the nucleation density can be reasonably attributed to the role of structural defects as nucleus. These structural defects are originated from the chain irregularity disrupted by the incorporation of ISB with bulky bicyclic asymmetric structure.

The spherulites of PDS have a needle-like structure developing radially and an extinction pattern in the form of a Maltese cross. Unfortunately, the lamellar growth seems to be less ordered and a two-arm extinction pattern is observed. And asymmetric spherulitic textures become more irregular and blurry with increasing  $T_c$  and ISB contents. It is difficult to obtain the radius of spherulites to safely measure their crystal growth rate. In addition, ring-banded spherulites are commonly observed in short chain aliphatic polyesters, such as poly(butylene succinate), poly(ethylene succinate) and their copolyesters [11-12]. Surprisingly, no evidence of ring-banded spherulites could be detected for this long chain PDS and its copolyesters in a wide temperature range even when very low supercoolings. Generally, ring-banded spherulites are believed to result from the twisting of lamellae. However, the exact origin of ring-banded spherulites is still uncertain, and the dependence of ring-banded spherulites of aliphatic polyester on the length of carbon chain is an open question[58]. The different morphology of long chain aliphatic polyesters in comparison with short chain analogs confirms their peculiar characteristics and suggests that further investigation into their crystalline structure and chain packing is required to better understand how a long chain sequence influences crystal morphology and thermal properties.

#### 4. Conclusions

In this work, biobased copolyesters poly(decamethylene sebacate-co-isosorbide sebacate) (P(DS-co-IS)) derived from biobased sebacic acid (SA), 1,10-decanediol (DD) and isosorbide (ISB) were prepared through a two-step melt polycondensation reaction. The effects of the incorporation of ISB and its content on nonthermal crystallization, isothermal crystallization kinetics, crystal structure, and spherulitic morphology of P(DS-co-IS) were investigated in detail with DSC, WAXD, and POM. Neat PDS displays high crystallization ability characteristics of long chain aliphatic polyester, due to the high flexibility of chains with long methylene sequences. Crystallization and thermal properties of the P(DS-co-IS) copolyesters, such as nonisothermal melt crystallization peak temperature and melting point, and the equilibrium melting point temperature, are significantly depressed by the incorporation of isosorbide with bulky rigid structure. However, the introduction of ISB segment does not change the crystal structure of P(DS-co-IS),

but decreases gradually the crystallinity. Isothermal crystallization kinetics of neat PDS and its copolyesters was further investigated. It is found that the crystallization mechanism remains unchanged for either neat PDS and P(DS-co-IS). However, the crystallization rates of P(DS-co-IS) decrease with increasing ISB composition and crystallization temperature, due to the more rigid structure than the methylene sequences. Thanks to the two competitive effects between the flexibility of long methylene sequences and the rigidity of isosorbide units, some peculiar characteristics are observed for neat PDS and P(DS-co-IS). In comparison with short chain aliphatic polyesters, single melting endotherm is found for this long chain PDS and its copolyesters, due to the formation of more perfect and stable crystals during isothermal crystallization process, however, no evidence of ring-banded spherulites could be detected for this long chain PDS and its copolyesters in a wide temperature range even when very low supercoolings.

## Acknowledgments

This work was financially supported by National Program on Key Basic Research Project (973 Program No. 2015CB654701) and National Science Foundation of China (Nos. 31000427, 21034001, and 21174021).

## Notes and references

1. A. Gandini. *Macromolecules*, 2008, 41, 9491-9504.
2. A. Gandini. *Green Chem*, 2011, 13, 1061-1083.
3. M. Singhvi, D. Gokhale. *RSC Adv.*, 2013, 3, 13558-13568.
4. R. Mülhaupt. *Macromol. Chem. Phys.*, 2013, 214, 159-174.
5. A. Tsui, Z. C. Wright, and C. W. Frank. *Annu. Rev. Chem. Biomol. Eng.*, 2013, 4, 143-170.
6. C. Vilela, A. F. Sousa, A. C. Fonseca, A. C. Serra, J. F. J. Coelho, C. S. R. Freire and A. J. D. Silvestre. *Polym. Chem.*, 2014, 5, 3119-3141.
7. X. Kong, H. Qi, J. M. Curtis. *J. Appl. Polym. Sci.*, 2014, 131, no. 40579.
8. Z. Gan, H. Abe, H. Kurokawa, and Y. Doi. *Biomacromolecules*, 2001, 2, 605-613.
9. G. Z. Papageorgiou, and D. N. Bikiaris. *Polymer*, 2005, 46, 12081-12092.
10. G. Z. Papageorgiou and D. N. Bikiaris. *Biomacromolecules*, 2007, 8, 2437-2449.
11. Y. Yang and Z. Qiu. *CrystEngComm*, 2011, 13, 2408-2417.
12. H. Wu and Z. Qiu. *CrystEngComm*, 2012, 14, 3586-3595.
13. F. Stempfle, P. Ortmann, S. Mecking. *Macromol. Rapid Commun.*, 2013, 34, 47-50.
14. R. T. Mathers. *J Polym Sci Part A: Polym Chem*, 2012, 50, 1-15.
15. N. Kolba, M. Winklera, C. Syldatk, M. A.R. Meier. *Eur Polym J*, 2014, 51, 159-166.

16. P. Ortmann and S. Mecking. *Macromolecules*, 2013, 46, 7213-7218.
17. F. Stempfle, B. S. Ritter, R. Mülhaupt and S. Mecking. *Green Chem.*, 2014, 16, 2008-2014.
18. L. Genovese, M. Gigli, N. Lotti, M. Gazzano, V. Siracusa, A. Munari, and M. D. Rosa. *Ind. Eng. Chem. Res.*, 2014, 53, 10965-10973.
19. Z. C. Liang, P. J. Pan, B. Zhu, T. Dong, L. Hua, and Y. Inoue. *Macromolecules*, 2010, 43, 2925-2932.
20. Z. C. Liang, P. J. Pan, B. Zhu, Y. Inoue. *Polymer*, 2011, 52, 2667-2676.
21. M. P. F. Pepels, M. R. Hansen, H. Goossens, R. Duchateau, *Macromolecules*, 2013, 46, 19, 7668-7677.
22. M. Soccio, N. Lotti, L. Finelli, M. Gazzano, A. Munari. *Polymer*, 2007, 48, 3125-3136.
23. C. Vilela, A. J. D. Silvestre and M. A. R. Meier. *Macromol. Chem. Phys.*, 2012, 213, 2220-2227.
24. P. Roesle, F. Stempfle, S. K. Hess, J. Zimmerer, C. RioBartulos, B. Lepetit, A. Eckert, P. G. Kroth, and S. Mecking. *Angew. Chem. Int. Ed.*, 2014, 53, 6800-6804.
25. A. K. Vasishtha, R. K. Trivedi, G. Das, *J Am Oil Chem Soc*, 1990, 67, 333-337.
26. H. Mutlu and M. A. R. Meier. *Eur. J. Lipid Sci. Technol.*, 2010, 112, 10-30.
27. H. Xu, Q. Zhou and J. Wang. *Chinese J Chem Eng*, 2013, 21, 967-973.
28. J. Tang, Z. Zhang, Z. Song, L. Chen, X. Hou, K. Yao. *Eur Polym J*, 2006, 42, 3360-3366.
29. J. Lee, M. K. Joo, H. Oh, Y. S. Sohn, B. Jeong, *Polymer*, 2006, 47, 3760-3766.
30. J. Kim, K. W. Lee, T. E. Hefferan, B. L. Currier, M. J. Yaszemski, L. Lu. *Biomacromolecules*, 2008, 9, 149-157.
31. J. P. Bruggeman, B-J de Bruin, C. J. Bettinger, R. Langer. *Biomaterials*, 2008, 29, 4726-4735.
32. Z. You, H. Cao, J. Gao, P. H. Shin, B. W. Day, Y. Wang. *Biomaterials*, 2010, 31, 3129-3138.
33. B. Guo, Y. Chen, Y. Lei, L. Zhang, W. Y. Zhou, A. B. M. Rabie, and J. Zhao. *Biomacromolecules*, 2011, 12, 1312-1321.
34. H. Park, J. Seo, H. Lee, H. Kim, I. B. Wall, M. Gong, J. C. Knowles, *Acta Biomaterialia*, 2012, 8, 2911-2918.
35. Y. Chandorkar, G. Madras and B. Basu. *J. Mater. Chem. B*, 2013, 1, 865-875.
36. D. J. Burke, T. Kawauchi, M. J. Kade, F. A. Leibfarth, B. McDearmon, M. Wolffs, P. H. Kierstead, B. Moon, and C. J. Hawker, *ACS Macro Lett.*, 2012, 1, 1228-1232.
37. F. Fenouillot, A. Rousseau, G. Colomines, R. Saint-Loup, J.-P. Pascault. *Prog. Polym. Sci.*, 2010, 35, 578-622.
38. M. Rose and R. a Palkovits. *ChemSusChem*, 2012, 5, 167-176.
39. H. R. Kricheldorf, S. M. Weidner. *Eur Polym J*, 2013, 49, 2293-2302.
40. H. S. Park, M. S. Gong and J. C. Knowles. *J Biomater Appl*, 2012, 27, 99-109.
41. C. Gioia, M. Vannini, P. Marchese, A. Minesso, R. Cavalieri, M. Colonna and A. Cellia. *Green Chem.*, 2014, 16, 1807-1815.

42. W. J. Yoon, S. Y. Hwang, J. M. Koo, Y. J. Lee, S. U. Lee, and S. S. Im. *Macromolecules*, 2013, 46, 7219-7231.
43. H. L. Kang, X. Li, J. J. Xue, L. Q. Zhang, L. Liu, R. W. Xu, B. C. Guo. *RSC Adv*, 2014, 4, 19462-19471.
44. H. Kang, M. Li, Z. Tang, J. Xue, X. Hu, L. Zhang and B. Guo. *J. Mater. Chem. B*, 2014, 2, 7877-7886.
45. D. Juais, A. F. Naves, C. Li, R. A. Gross, and L. H. Catalani. *Macromolecules*, 2010, 43, 10315-10319.
46. F. Pion, P. H. Ducrot, F. Allais. *Macromol. Chem. Phys.*, 2014, 215, 431-439.
47. M. Z. Oulame, F. Pion, S. Allauddin, K. V. S. N. Raju, P. H. Ducrot, F. Allais. *Eur Polym J*, 2015, 63, 186-193.
48. I. Barbara, A. L. Flourat, F. Allais. *Eur Polym J*, 2015, 62, 236-243.
49. G. Z. Papageorgiou, D. N. Bikiaris, D. S. Achilias, S. Nanaki. *J Polym Sci Part B: Polym Phys*, 2010, 48, 672-686.
50. A. Díaz, L. Franco, J. Puiggali. *Thermochimica Acta*, 2014, 575, 45-54.
51. C. Tsai, W. Chang, C. Chen, H. Lu, M. Chen. *Eur Polym J*, 2008, 44, 2339-2347.
52. C. Chen, J. Peng, M. Chen, H. Lu, C. Tsai, C. Yang. *Colloid Polym Sci*, 2010, 288, 731-738.
53. C. Berti, A. Celli, P. Marchese, G. Barbiroli, F. Di. Credico, V. Verney, S. Commereu. *Eur Polym J*, 2009, 45, 2402-2412.
54. M. J. Avrami. *J Chem Phys*, 1940, 8, 212-224.
55. S. Gupta, X. Yuan, T.C.M. Chung, M. Cakmak, R.A. Weiss. *Polymer*, 2014, 55, 924-935.
56. J. D. Hoffman, J. J. Weeks. *J Res Natl Bur Stand Sect A*, 1965, 66, 13-28.
57. P. Marchese, E. Marianucci, G. Barbiroli, F. Di. Credico. *e-Polymers*, 2007, no. 057
58. A. Celli, G. Barbiroli, C. Berti, D. C. Francesco, C. Lorenzetti, P. Marchese, E. Marianucci, *J Polym Sci Part B: Polym Phys*, 2007, 45, 1053-1067.